Journal of Sol-Gel Science and Technology (2023) 108:609–620
https://doi.org/10.1007/s10971-023-06227-2

ORIGINAL PAPER: NANO-STRUCTURED MATERIALS (PARTICLES, FIBERS, COLLOIDS, COMPOSITES, ETC.)

Effect of the alumina and silica source mixing procedure on the microstructural evolution of alumina-mullite composite fibers prepared by sol–gel method

Qiang Liu[1] · Lingjiao Zhan[1] · Chaozhong Wu[1] · Haotian Liu[1] · Wensheng Liu[1] · Shuwei Yao[1] · Yunzhu Ma[1]

Published online: 21 September 2023

Abstract

The preparation of precursor sol is the first and crucial step in fabricating oxide fibers by the sol–gel method. In this study, different aluminum-silica sols were prepared by adjusting the alumina and silica source mixing procedure using aluminum carboxylate sol and tetraethoxysilane (TEOS) as the aluminum source and silicon source, respectively. Continuous alumina-mullite precursor fibers were obtained by dry spinning and the effects of alumina and silica source mixing procedure on the phase transition and microstructure evolution of alumina-mullite composite fibers were investigated. The results showed that the mullite formation temperature in the fibers obtained by adding TEOS during the preparation of aluminum carboxylate sol was about 1300 °C, while it was 800 °C in the fibers obtained by mixing aluminum carboxylate sol and TEOS. In addition, the grain size of the fibers obtained by adding TEOS during the preparation of aluminum carboxylate sol was significantly smaller than that obtained by mixing aluminum carboxylate sol and TEOS. The mechanism of this difference was that the aluminum-silica sol obtained by adding TEOS during the preparation of aluminum carboxylate sol was a diphasic sol, while the aluminum-silica sol obtained by adding TEOS in the prepared aluminum carboxylate sol was a monophasic sol.

Graphical Abstract

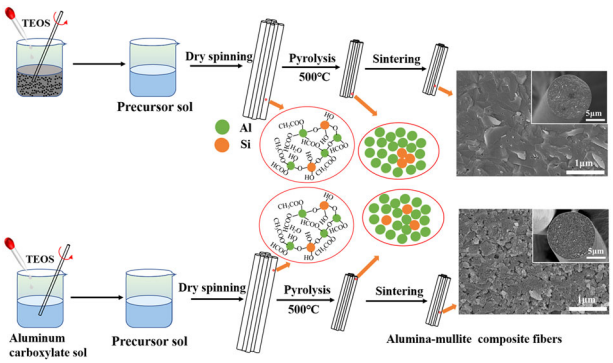

Keywords Sol–gel method · Alumina-mullite composite fibers · Phase transformation · Microstructural evolution

✉ Shuwei Yao
shwyao@csu.edu.cn

✉ Yunzhu Ma
zhuzipm@csu.edu.cn

[1] National Key Laboratory of Science and Technology on High-strength Structural Materials, Central South University, Changsha 410083, China

Highlights

- Different alumina-mullite fibers precursor sols were prepared by adjusting the alumina and silica source mixing procedures.
- The phase transformation and microstructural evolution of alumina-mullite composite fibers obtained by different alumina and silica source mixing procedures were investigated systematically.
- The grain size of the fibers obtained by adding TEOS during the preparation of aluminum carboxylate sol was significantly smaller than that obtained by mixing aluminum carboxylate sol and TEOS.

1 Introduction

During the past few decades, with the vigorous development of aviation, aerospace, military and other technical fields, the demand for high-performance ceramic fibers has increased rapidly [1–4]. Compared with carbon fibers or other non-oxide fibers, alumina-based fibers have attracted much attention due to their low density, strong oxidation resistance and stable chemical properties [5–7]. Based on the excellent properties of alumina-based fibers, many different types of commercial alumina-based fibers have been developed and marketed by foreign companies. The most successful and widely used is the Nextel^{TM} series of alumina-based fibers produced by 3 M company [8]. In the Nextel^{TM} series, the Nextel^{TM} 720 alumina-mullite fibers composed of 85 wt.% Al_2O_3 and 15 wt.% SiO_2 have excellent creep resistance and are the first choice for high-temperature service, with a long-term stable service temperature up to 1100 °C [9]. The grains size of mullite in Nextel^{TM} 720 fibers is about 500 nm, and the grains size of α-Al_2O_3 is 70 nm. Due to the size and morphology of mullite grains, Nextel^{TM} 720 fibers can inhibit the slip of grain boundary at high temperature and has excellent creep resistance [10].

There are several methods to prepare alumina-mullite composites, such as melting method, infiltration process, sol–gel method and so on [11–13]. The sol–gel process has become the preferred method for preparing alumina-based fibers due to its mild reaction conditions, high product uniformity and high purity [14]. In the process of preparing fibers by sol–gel method, the precursor sol is obtained by hydrolysis and polymerization of the reactants, and then the precursor sol is concentrated to obtain a suitable spinning viscosity, and the gel fibers were prepared by dry or wet spinning. Subsequently, the excess material in the precursor fibers is removed by low-temperature pyrolysis, and the ceramic fibers are obtained by high-temperature sintering [15]. The preparation of precursor sol is the first and crucial step in the preparation of alumina-based fibers, which directly affects the behavior of fibers at high temperature, such as phase composition, phase transition temperature, phase transition path and microstructures [16].

Many researchers used TEOS and aluminum nitrate as raw materials to prepare alumina-mullite composites by sol–gel method, and sintered at about 1000 °C to obtain ceramics with mullite as the only phase [17]. Chakraborty et al. [18] prepared mullite using TEOS and aluminum nitrate as raw materials. It was found that the ceramic composed of mullite and spinel was obtained after sintering at 1000 °C, and the pure mullite phase was only sintered above 1250 °C. The difference was that the reaction temperature used was 80 °C, while the commonly used reaction temperature was 60 °C. In addition, different raw materials also affect the phase transition and microstructures. Sedaghat et al. [19] studied the effects of different silicon sources on the preparation of alumina-mullite composites by sol–gel method using aluminum chloride, silica sol, TEOS and ethanol as raw materials. Compared with alumina-mullite composites obtained by silica sol as silicon source, the relative density and average grain size of alumina-mullite composites obtained by tetraethyl orthosilicate as silicon source increased and accelerated. Dong et al. [20] synthesized diphasic mullite sol by using polymethyl siloxane and aluminum sec-butoxide as raw materials, and successfully prepared mullite nanofibers. γ-Al_2O_3 appeared in mullite nanofibers at 1000 °C, mullite was formed at 1200 °C, and the corresponding grain size of nanofibers was about 100 nm after sintering at 1500 °C. Wu et al. [21, 22] prepared mullite nanofibers by monophasic precursor sol electrospinning using aluminum isopropoxide, aluminum nitrate and polymethyl siloxane as raw materials. The results showed that the mullite phase was directly formed by the amorphous phase at 980 °C. The grain size of mullite nanofibers sintered at 1200 °C was about 100 nm, but the grain size grew obviously after sintering at higher temperatures.

From the above studies, there have been many and sufficient studies on the influence of precursor sol on alumina-mullite composites or mullite nanofibers. However, the effect of precursor sol difference on the phase transformation and microstructure of continuous alumina-mullite composite fibers has not been reported. Therefore, in this study, different aluminum-silica sols were prepared by adjusting the mixing procedures of Al and Si by using aluminum carboxylate sol and TEOS as the aluminum source and silicon source, respectively. Continuous alumina-mullite precursor fibers were obtained by dry spinning. The effects of Al and Si mixing procedures on the

phase transition and microstructure evolution of alumina-mullite composite fibers were investigated.

2 Experimental

2.1 Preparation process of fibers

The alumina-mullite composite fibers precursor sols were prepared using aluminum powder, formic acid (HCOOH), acetic acid (CH_3COOH), nitric acid (HNO_3) and tetraethoxysilane ($C_8H_{20}O_4Si$, TEOS) as raw materials. Two types of alumina-mullite composite fibers precursor sols were prepared by adjusting the mixing procedures of Si and Al, which were pre-addition and post-addition, respectively. The pre-addition of TEOS was as follows: Aluminum powder, formic acid, acetic acid, nitric acid and deionized water were placed in a water bath reactor, the molar ratio of Al: HCOOH: CH_3COOH: HNO_3: H_2O was 1:0.67:0.6:0.35:30. After stirring at 90 °C for 1 h, TEOS was added dropwise, and the stirring reaction was continued until the aluminum powder was fully dissolved, the generated gas was discharged by the condensation tube. The sol was filtered by vacuum filtration at a pressure of 3000 Pa, and the filter paper pore size was 0.7 μm. After filtering the impurities, an aluminum-silica sol with a mass ratio of Al_2O_3 to SiO_2 of 85: 15 was obtained, which was recorded as AM-1 sol. The post-addition of TEOS was as follows: The corresponding mass aluminum powder, formic acid, acetic acid, nitric acid and deionized water were weighed and placed in a water bath reactor. The reaction was stirred in a water bath at 90 °C until the aluminum powder was fully dissolved. After filtering the impurities, the aluminum carboxylate sol was obtained. Then, the appropriate amount of aluminum carboxylate sol was placed in a beaker, the weighed TEOS was added, the mouth of the bottle was sealed and the sol was stirred. After stirring for 12 h at room temperature, the aluminum-silica sol with a mass ratio of Al_2O_3: SiO_2 of 85: 15 was obtained, which was recorded as AM-2 sol. Figure 1 shows the overall manufacturing process.

2.2 Spinning of precursor fibers

In order to obtain a sol suitable for spinning, polyvinylpyrrolidone (PVP) was used as a spinning aid, and the addition amount was 5 wt.%. After stirring for 1 h, The sol was concentrated on a rotary evaporator to remove the excess solvent to a sui‘ viscosity for spinning (40–60 Pa·s). The concentration process temperature was 50 °C, the rotation speed was 50 r/min, and the vacuum degree was 30 Pa. Then continuous alumina-mullite precursor fibers were fabricated by a dry spinning device. In the spinning process, 0.6 MPa gas was used as the injection force, the diameter of spinneret was 80 μm, the number of holes was

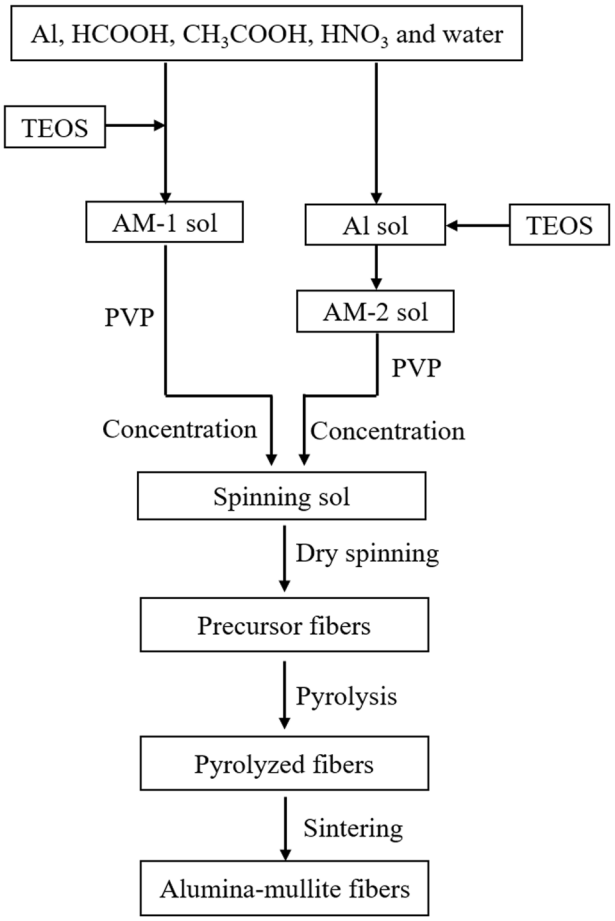

Fig. 1 The process of preparing aluminum-silica sol and fibers by different TEOS introduction procedures, AM-1 sol was the aluminum-silica sol prepared by adding TEOS during the preparation of aluminum carboxylate sol, AM-2 sol was the aluminum-silica sol prepared by mixing the prepared aluminum carboxylate sol with TEOS

100, the temperature in the spinning tunnel was set at 40–100 °C, and the rate of fibers collection was 120 m/min. The spun alumina-mullite precursor fibers were stored in a constant temperature and humidity box at 25 °C.

2.3 Pyrolysis and sintering

Precursor fibers were pyrolyzed in a muffle furnace in the air to remove water and organic components to obtain the pyrolyzed fibers. The precursor fibers were placed in a corundum burner, and the sample was pyrolyzed in the middle of the muffle furnace in order to be heated evenly. The heating rate of the pyrolysis process was as follows: 3 K/min from room temperature to 100 °C, followed by 5 K/min to 400 °C, then finally 3 K/min to 500 °C and held for 30 min, and finally cooled with the furnace. To receive alumina-mullite fibers, the pyrolyzed fibers were sintered in a high-temperature tube furnace in the air at 800–1400 °C for a certain time. After sintering, the fibers were directly taken out and cooled at room temperature.

2.4 Characterization of fibers

The morphology of the obtained sol was characterized by Titan G2 60–300 (FEI, USA) spherical aberration corrected transmission electron microscope (TEM) with an acceleration voltage of 300 kV. The particle size of the obtained precursor sol was tested by Zetasizer Nano ZS (Malvern, UK) nanoparticle size analyzer. The ^{27}Al and ^{29}Si NMR of the precursor sol were tested by Ascend-400 (Bruker, German) nuclear magnetic resonance spectrometer. The FT-IR spectroscopy of the fibers was characterized by Nicolet 6700 (Thermo, USA) infrared spectrometer, the fibers were ground into powder and pressed with KBr, the wavenumber range of scanning was 2500–400 cm^{-1}. The phase composition of the fibers was analyzed by D8 ADVANCE (Bruker, German) X-ray diffractometer, the light source of the equipment was CuKα ray, the scanning speed was 0.5 °/min, and the scanning range was $10° < 2\theta < 80°$. The morphology of the fibers was analyzed using a Regulus 8230 (Hitach, Japan) cold field emission scanning electron microscope (SEM). The tensile strength of the fibers was tested at room temperature using a fiber strength tester (XS(08)XT-3, Xu Sai, China) at a speed of 1 mm/min. The gauge length of the fiber for tensile testing was 15 mm. A total of 20 samples were tested for strength, and the diameter of each fiber was measured by SEM.

3 Results

Aluminum carboxylate sol and aluminum-silica sol obtained by different Al-Si mixing methods were characterized by TEM and laser particle size analyzer, respectively, to analyze the effects of different aluminum-silicon mixing procedures on the morphology and size of the precursor sol. The relevant results are shown in Fig. 2. As can be seen from Fig. 2a–c, the particles of the three sols are spherical with uniform size distribution, and no particle agglomeration occurs. The average particle sizes of the three sols obtained by laser particle size analyzer (Fig. 2d) were 5.1, 6.8 and 5.9 nm, respectively. From the above characterization, it can be seen that the morphology of AM-1 sol and AM-2 sol was not much different from that of aluminum carboxylate sol, indicating that the pre-addition and post-addition of TEOS can be well mixed with aluminum carboxylate sol to form alumina-mullite precursor sol with uniform size. The difference was the particle size, the addition of TEOS increased the particle size of sol, and the size of the sol obtained by the pre-addition method of TEOS was larger.

Figure 3 shows the ^{27}Al NMR and ^{29}Si NMR spectra of the three sols. It can be seen from Fig. 3a that the aluminum carboxylate sol has three chemical shift peaks at 0.7 ppm, 5.4 ppm and 77 ppm. The peak at 0.7 ppm was assigned to the AlO_6 monomer such as $[Al(H_2O)_6]^{3+}$, $[Al(HCOO)(H_2O)_6]^{2+}$, $[Al(CH_3COO)(H_2O)_6]^{2+}$ [23]. The peak at 5.4 ppm was assigned to the AlO_6 oligomer such as Al_{13}, and the peak at 77 ppm was assigned to the AlO_4 structure in the aluminum polymer. When TEOS was added to form AM-1 sol during the preparation of aluminum carboxylate sol, it can be seen that the peak intensity of AlO_6 monomer increased, and the peak shift of AlO_4 structure in the sol was 83 ppm. The peak intensity of AlO_6 monomers in AM-2 sol was further enhanced, and the peak intensity of AlO_6 oligomers was reduced. The results indicated that the addition of TEOS promotes the formation of AlO_6 monomers in the aluminum-silicon sol, and the aluminum-silicon sol obtained by the post-addition procedure of TEOS was more obvious. Figure 3b shows the ^{29}Si NMR spectra of the two alumina-mullite precursor sols. It can be seen that the chemical structure of silicon in the two precursor sols was not much different, and peaks appeared at the chemical shifts of −81, −83 and −91 ppm. The peak at −81 ppm was attributed to the connection of silicon atoms with four hydroxyl groups ($Si(OH)_4$) [24], the peak at −83 ppm was attributed to the connection of silicon atoms with three hydroxyl groups ($[SiO(OH)_3]^-$), and the peak at −91 ppm was attributed to the connection of silicon atoms with two hydroxyl groups ($[SiO_2(OH)_2]^{2-}$). The peak proportion of −81 ppm in both precursor sols was the highest, indicating that silicon in the two precursor sols mainly exists in the form of $Si(OH)_4$. In addition, the peak intensity of $[SiO(OH)_3]^-$ and $[SiO_2(OH)_2]^{2-}$ in AM-2 sol was higher than that in AM-1 sol, indicating that there is a certain amount of $[SiO(OH)_3]^-$ and $[SiO_2(OH)_2]^{2-}$ in AM-2 sol.

Both AM-1 and AM-2 precursor sols could be concentrated to a suitable viscosity to fabricated continuous alumina-mullite precursor fibers by dry spinning. Figure 4 is the morphology of precursor fibers spun by different precursor sols. It can be seen that the surface of the two spinning precursor fibers was smooth, without defects such as pores and cracks, and the diameter distribution was uniform. The diameters of AM-1 fibers and AM-2 fibers were 17.08 ± 1.05 μm, 15 ± 0.52 μm, respectively.

Through the above results, it can be seen that the aluminum-silica sols with uniform size were obtained by pre-addition and post-addition of TEOS. In terms of chemical structure, alumina in the precursor sol obtained by the pre-adding TEOS procedure mainly exists in the form of AlO_6 oligomers, and silicon mainly exists in the form of $Si(OH)_4$. In the precursor sol obtained by the post-adding TEOS procedure, aluminum mainly exists in the form of AlO_6 monomers, silicon mainly exists in the form of $Si(OH)_4$, and a small part exists in the form of $[SiO(OH)_3]^-$ and $[SiO_2(OH)_2]^{2-}$.

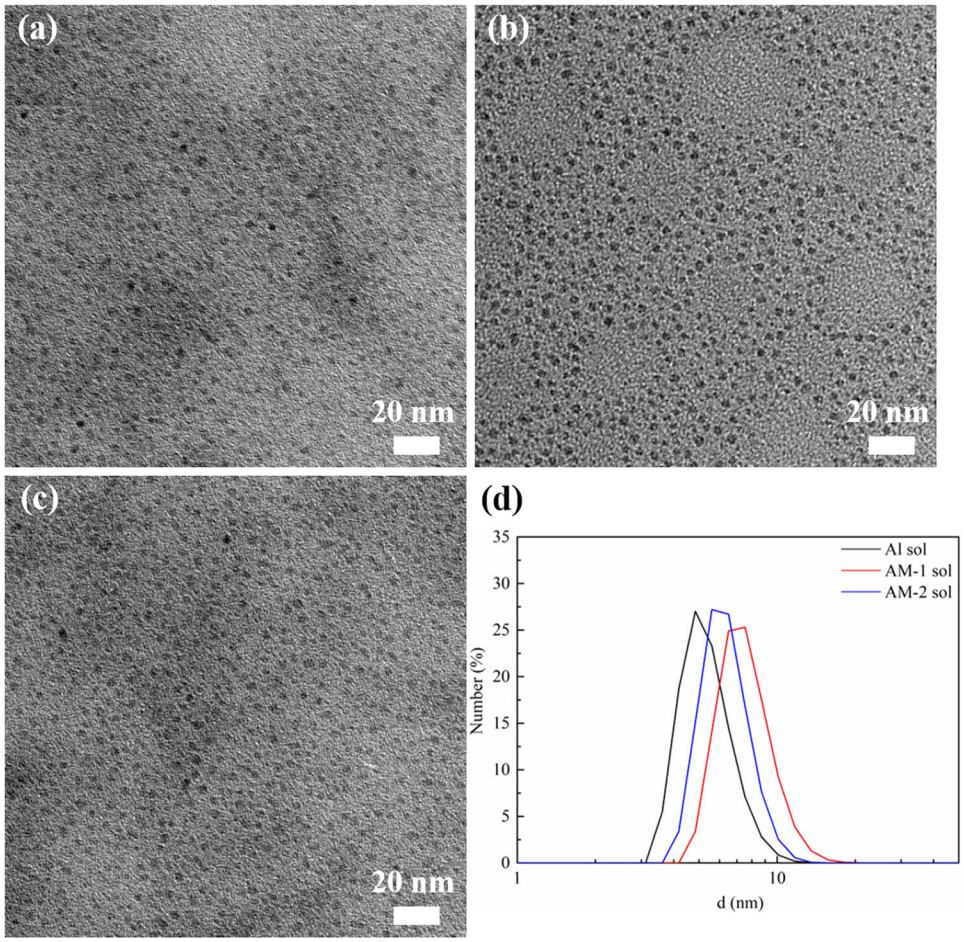

Fig. 2 TEM images and particle size distribution of precursor sol, **a** aluminum carboxylate sol, **b** AM-1 sol, **c** AM-2 sol, **d** particle size distribution

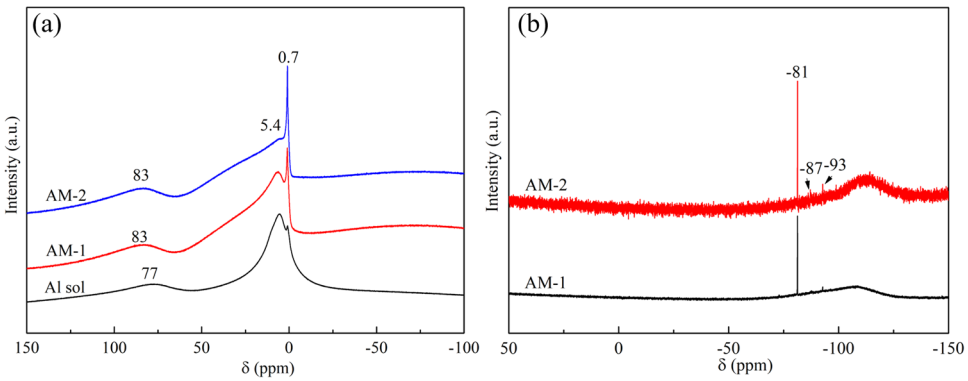

Fig. 3 ^{27}Al NMR and ^{29}Si NMR spectra of aluminum-silica sols with different TEOS addition procedures. **a** ^{27}Al NMR, **b** ^{29}Si NMR

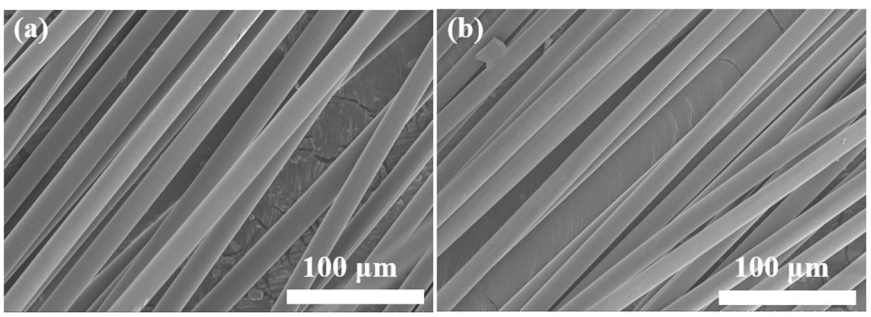

Fig. 4 Morphology of alumina-mullite precursor fibers obtained by different precursor sols, **a** AM-1, **b** AM-2

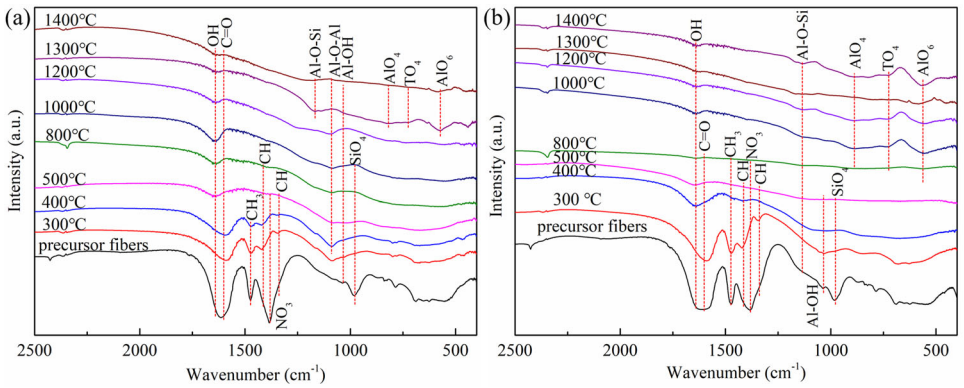

Fig. 5 FT-IR of fibers spun by different TEOS addition procedures at different heat treatment temperatures. **a** AM-1 fibers, **b** AM-2 fibers

In order to compare the structural changes of the two fibers during pyrolysis and sintering, the fibers after heat treatment at different temperatures for 1 h were characterized by FT-IR. The results are shown in Fig. 5. It can be seen that both AM-1 and AM-2 precursor fibers contain obvious vibration peaks of organic and inorganic groups. The difference is that AM-2 precursor fibers has a stretching vibration peak belonging to Al-O-Si linkages at 1180 cm^{-1} [25], while AM-1 precursor fibers does not appear, indicating that the mixed scale of aluminum and silicon in the AM-2 precursor sol was atomic scale. In the pyrolysis stage before 500 °C, the vibration peak intensity of -OH, $-CH_3$, NO_3^- and other groups in the vicinity of 1300–1700 cm^{-1} of AM-1 and AM-2 fibers gradually weakened with the increase of temperature, and basically disappeared at 500 °C, indicating that the organic and inorganic groups in the fibers have been removed. In addition, after pyrolysis at 300 °C, the stretching vibration peak of Si-O-Si linkages appeared in AM-1 fibers at 1087 cm^{-1}, but not in AM-2 fibers.

In the sintering stage above 500 °C, with the increase of sintering temperature, the stretching vibration peak of Al-O-Al linkages at 1087 cm^{-1} in AM-1 fibers disappeared at 1300 °C. At the same time, the bending vibration of T-O-T (TO_4, T = Al or Si) linkages and the stretching vibration peak of Al-O-Si linkages appeared at 740 and 1180 cm^{-1}, and the vibration peaks of AlO_4 and AlO_6 disappeared during pyrolysis also appeared again. For AM-2 fibers, the vibration peaks of T-O-T, AlO_4 and AlO_6 appeared after sintering at 1000 °C. It can be seen from the FT-IR results that the different introduction methods of TEOS have little effect on the removal of substances in the pyrolysis process of precursor fibers, mainly on the chemical structure evolution of the fibers. The vibration peaks of Al-O-Si and TO_4 appeared in AM-1 fibers after sintering at 1300 °C, while the vibration peak of Al-O-Si and TO_4 appeared in AM-2 fibers after sintering at 1000 °C, suggesting that the crystallization temperature of mullite in AM-1 fibers was about 1300 °C, and that in AM-2 fibers was about 1000 °C.

The phase transition process of alumina-mullite composite fibers with different TEOS addition procedures was further analyzed by XRD. As shown in Fig. 6, it can be found that the AM-1 and AM-2 fibers after pyrolysis at 500 °C were amorphous. The diffraction characteristic peaks of γ-Al_2O_3 appeared in AM-1 fibers after 800 °C, and the diffraction characteristic peaks intensity of γ-Al_2O_3 increased with the increase of sintering temperature. After sintering at 1300 °C, the diffraction characteristic peaks of γ-Al_2O_3 in AM-1 fibers disappeared, and the characteristic peaks of mullite and α-Al_2O_3 appeared. From the $2\theta = 25–27$ ° enlarged figure in Fig. 6b, the formed mullite was stable orthorhombic mullite (aluminum-poor mullite) [26]. Before sintering at 1300 °C, there was no diffraction characteristic peak of SiO_2 in AM-1 fibers. Only amorphous peak was observed at $2\theta = 20°$, which was attributed to the characteristic peak of amorphous SiO_2. It showed that the mullite in AM-1 fibers was formed by the reaction of amorphous SiO_2 and γ-Al_2O_3 [27]. For AM-2 fibers (Fig. 6c), the characteristic peaks of mullite appeared after sintering at 800 °C. It can be found from Fig. 6d that the generated mullite was metastable tetragonal mullite (aluminum-rich mullite). Before 1200 °C, the diffraction characteristic peaks intensity of tetragonal mullite increased with the increase of sintering temperature. At 1300 °C, the diffraction characteristic peaks of α-Al_2O_3 appeared in AM-2 fibers. After sintering at 1400 °C, tetragonal mullite transformed into orthorhombic mullite.

In order to further clarify the difference of phase transition paths between AM-1 and AM-2 fibers, the fibers sintered at 1400 °C for a different time were analyzed by XRD. As shown in Fig. 7a, the diffraction characteristic peaks of γ-Al_2O_3 appeared after AM-1 fibers was sintered at 1400 °C for 1 min, and it was the only phase. The diffraction characteristic peaks of mullite appeared after sintering at 1400 °C for 5 min. From the $2\theta = 25–27°$ enlarged figure in Fig. 7b, it can be determined that the formed mullite was stable orthorhombic mullite. When the sintering time was extended to 10 min, the diffraction characteristic peaks of θ-Al_2O_3 and α-Al_2O_3 appeared in addition to the diffraction

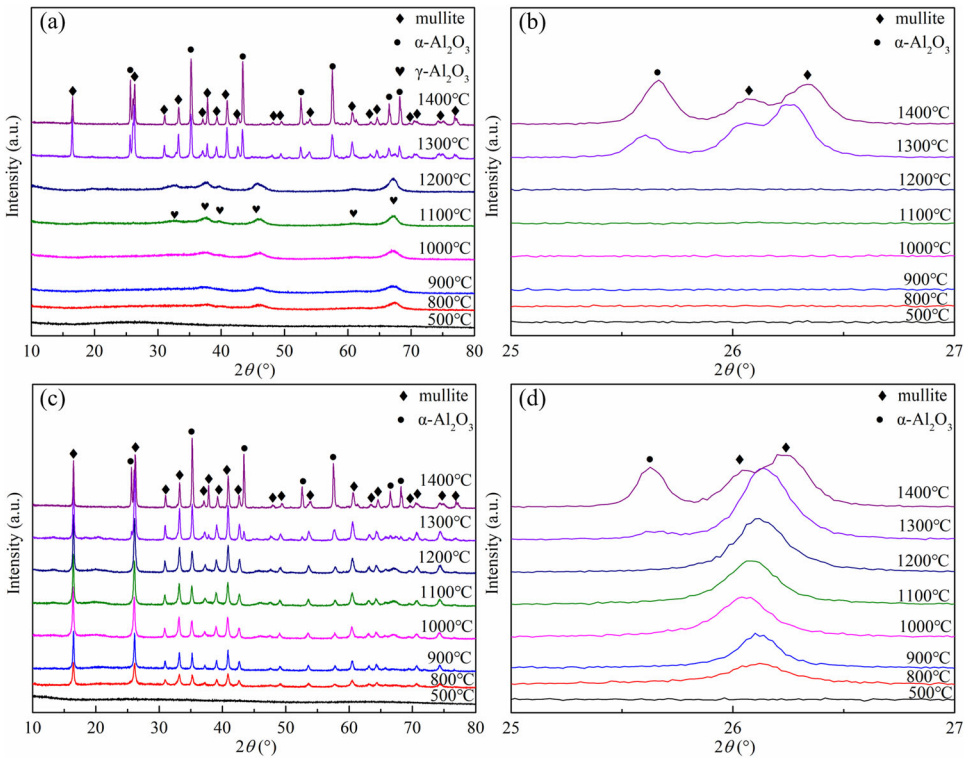

Fig. 6 XRD patterns of fibers after sintering at different temperatures for 1 h. **a**, **b** AM-1 fibers, **c**, **d** AM-2 fibers

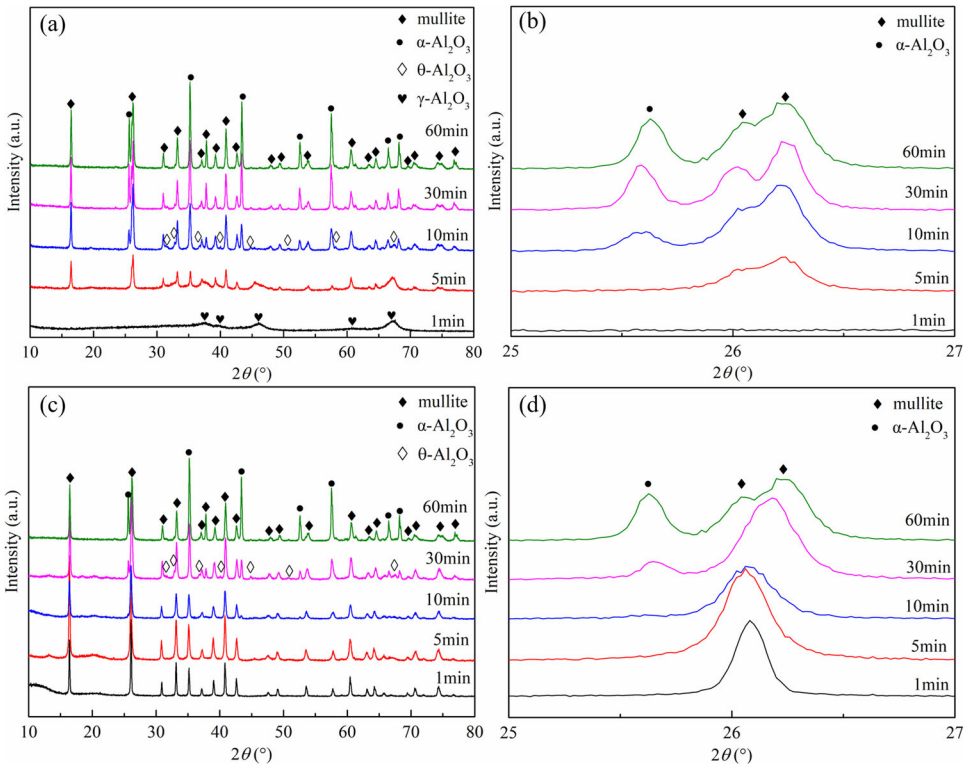

Fig. 7 XRD patterns of fibers sintered at 1400 °C for different time. **a**, **b** AM-1 fibers; **c**, **d** AM-2 fibers

characteristic peaks of mullite. After sintering for 30 min, the diffraction characteristic peaks of θ-Al_2O_3 disappeared, and only the diffraction characteristic peaks of α-Al_2O_3 and mullite remained. For AM-2 fibers, it can be found from Fig. 7c, d that the diffraction characteristic peak of tetragonal mullite appeared after sintering at 1400 °C for 1 min. When the sintering time was extended to 30 min, the diffraction characteristic peaks of θ-Al_2O_3 and α-Al_2O_3

appeared in the AM-2 fibers. After sintering for 60 min, the diffraction characteristic peaks of θ-Al_2O_3 disappeared, and the mullite in the fibers changed from a tetragonal structure to an orthorhombic structure.

From the above XRD results, it can be seen that the phase transition path of AM-1 fibers obtained by adding TEOS in the preparation process of the aluminum sol was: Amorphous → γ-Al_2O_3 → γ-Al_2O_3 + orthorhombic mullite → θ-Al_2O_3 + α-Al_2O_3 + orthorhombic mullite → α-Al_2O_3 + orthorhombic mullite; the phase transition path of AM-2 fibers obtained by mixing the alumina sol and TEOS was: Amorphous → tetragonal mullite → θ-Al_2O_3, α-Al_2O_3, tetragonal + mullite → α-Al_2O_3 + orthorhombic mullite.

The AM-1 and AM-2 fibers sintered at 1200–1400 °C for 1 h were characterized by SEM to analyze the effect of different TEOS introduction procedures on the microstructure evolution of alumina-mullite composite fibers. As shown in Fig. 8a, after sintering at 1000 °C or 1200 for 1 h, the AM-1 fibers have a fine grain size of about 20 nm with a dense structure, and no pores were observed. It can be seen that when the temperature increased to 1300 °C, grain with a size of about 200 nm appeared in AM-1 fibers (Fig. 8c), and there were also grains with a size of less than 100 nm. Combined with XRD patterns (Fig. 6a), it can be known that the large grains were mullite grains. The average grain size of AM-1 fibers sintered at 1400 °C was about 500 nm, and the grain size of 100 nm can also be observed. The internal structure of the fiber was still dense, and pores caused by grain growth could also be observed inside the grains. Different from AM-1 fibers, the average grain size of AM-2 fibers was about 100 nm after sintering at 1000 °C for 1 h, and the average grain size increased to about 400 nm after sintering at 1200 °C for 1 h. After sintering at 1300 °C, the average grains size has exceeded 1μm. The average grain size of AM-2 fibers sintered at 1400 °C for 1 h was decreased, but many pores could be observed inside the fibers, which was caused by the transformation of tetragonal mullite into orthorhombic mullite. By comparing the fracture morphologies of AM-1 fibers and AM-2 fibers during high-temperature sintering, it can be found that the AM-1 fibers obtained by pre-addition of TEOS could effectively inhibit the growth of grain at the high-temperature sintering process. However, the average grains size of the AM-2 fibers obtained by the post-addition of TEOS procedure after sintering at 1300 °C for 1 h has exceeded 1 μm.

In order to compare the effect of silicon addition procedure on the properties of alumina-mullite composite fibers, the mechanical properties of two groups of pyrolyzed fibers obtained by different silicon addition methods were tested after sintering at 1400 °C for 5 min. Figure 9 shows the average monofilament tensile strength of the sintered fibers. Among the two groups of sintered fibers, AM-1 fibers showed the best performance, and the tensile strength reached 1.52 ± 0.13 GPa, while the tensile strength of AM-2 fibers was only 0.51 ± 0.17 GPa.

4 Discussion

When aluminum powder and formic acid, acetic acid, nitric acid in an aqueous solution in the preparation of aluminum carboxylate sol, aluminum powder first with H_3O^+ and H_2O to obtain hydrated aluminum ions, and then hydrolysis, which could be expressed by the following reaction equation:

$$6H_3O^+ + H_2O + 2Al \rightarrow Al(H_2O)_6^{3+} + 3H_2 \uparrow \quad (1)$$

$$Al(H_2O)_6^{3+} + H_2O \rightarrow Al(OH)(H_2O)_5^{2+} + H_3O^+ \quad (2)$$

$$Al(OH)(H_2O)_5^{2+} + H_2O \rightarrow Al(OH)_2(H_2O)_4^{+} + H_3O^+ \quad (3)$$

The pH of the aluminum carboxylate sol obtained after the reaction was 3.8. According to relevant literature reports [28, 29], when the reaction environment pH of the sol system was $3 < pH < 4.3$, $Al(OH)(H_2O)_5^{2+}$ was the preferred product after the aluminum powder was dissolved in formic acid, acetic acid and nitric acid aqueous solution. At the same time, there was a certain amount of hydrated aluminum ions such as $Al(H_2O)_6^{3+}$ and $Al(OH)_2(H_2O)_4^{+}$. Then carboxylate ions further replace the coordinated water in $Al(OH)(H_2O)_5^{2+}$ and $Al(H_2O)_6^{3+}$ to form different carboxylate aluminum salts or ions. The generated carboxylate aluminum salts or ions were continuously polymerized to form AlO_6 polymers with different degrees of polymerization. The possible polymerization reactions are as follows:

$$Al(H_2O)_6^{3+} + HCOO^- + H_3CCOO^- \rightarrow Al(O_2CH)(O_2C_2H_3)(H_2O)_4^+ + 2H_3O^+ \quad (4)$$

$$2\left[Al(O_2CH)(O_2C_2H_3)(H_2O)_4\right]^+ \rightarrow \left[Al_2(OH)_2(O_2CH)(O_2C_2H_3)_2(H_2O)_6\right]^+ + HCOOH + H_3O^+ \quad (6)$$

$$3\left[Al(O_2CH)(O_2C_2H_3)(H_2O)_4\right]^+ \rightarrow \left[Al_3(OH)_3(O_2CH)_2(O_2C_2H_3)_3(H_2O)_9\right]^+ + HCOOH + 2H_3O^+ \quad (7)$$

$$6\left[Al(O_2CH)(O_2C_2H_3)(H_2O)_4\right]^+ \rightarrow \left[Al_6(OH)_{10}(O_2CH)_3(O_2C_2H_3)_3(H_2O)_{14}\right]^{2+} + 3HCOOH + 3CH_3COOH + 4H_3O^+ \quad (8)$$

$$13\left[Al(O_2CH)(O_2C_2H_3)(H_2O)_4\right]^+ \rightarrow \left[Al_{13}(O)_4(OH)_{12}(O_2CH)_6(O_2C_2H_3)_7(H_2O)_{18}\right]^{6+} + 7HCOOH + 6CH_3COOH + 8H_2O + 7H_3O^+ \quad (9)$$

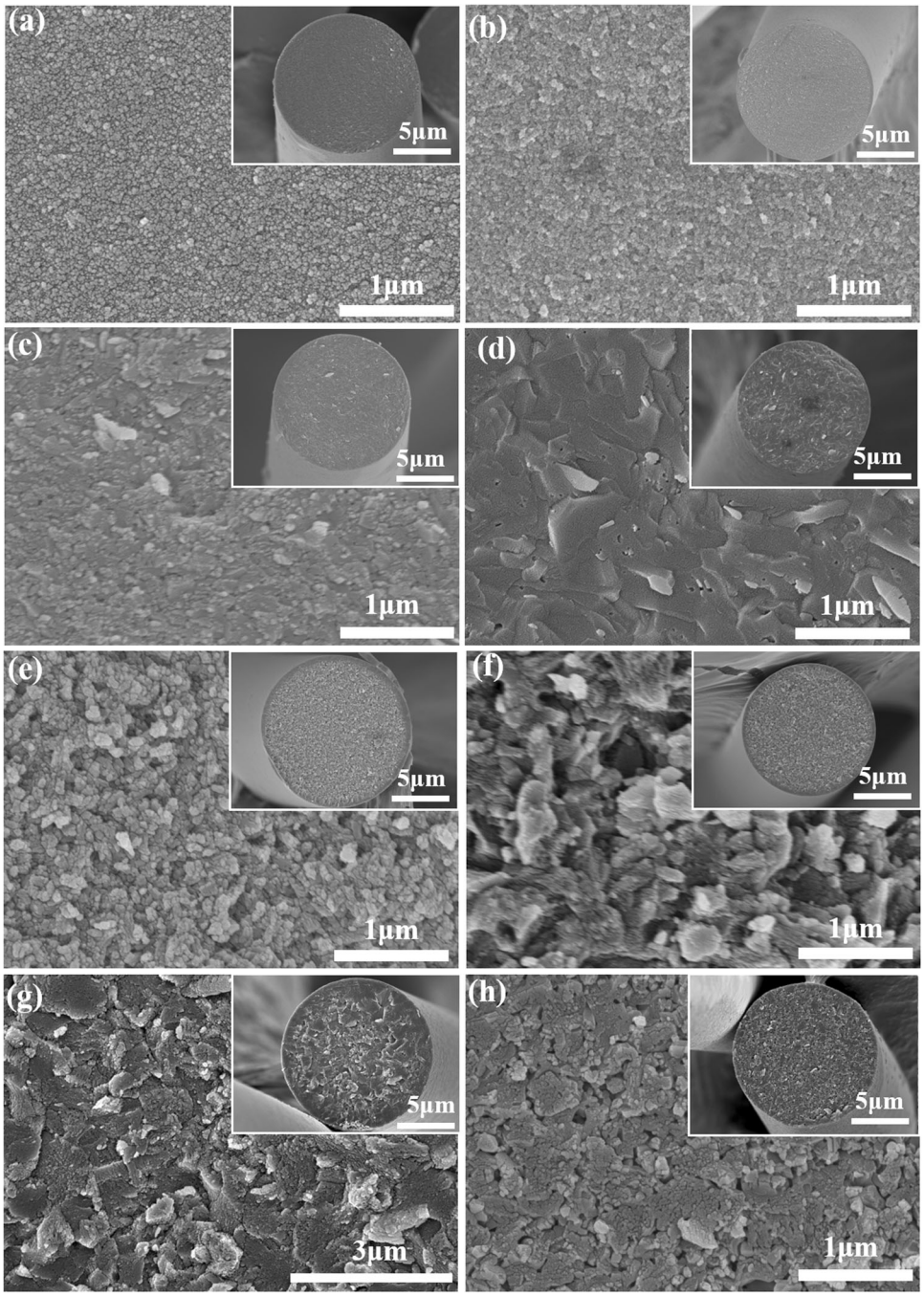

Fig. 8 SEM images of fracture morphologies of AM-1 and AM-2 fibers sintered at different temperatures for 1 h. **a**–**d** were the fracture morphologies of AM-1 fibers sintered at 1000, 1200, 1300 and 1400 °C for 1 h, respectively, **e**–**h** were the fracture morphologies of AM-2 fibers sintered at 1000, 1200, 1300 and 1400 °C for 1 h, respectively

For TEOS, it can be hydrolyzed by acid catalysis or alkali catalysis [30, 31]. The acid-catalyzed hydrolysis reaction process can be explained by the electrophilic reaction mechanism, that is, the positively charged hydrated hydrogen ion (H_3O^+) in the solution was easy to attack the Si atom with more OR groups, forming an intermediate transition state that H_3O^+ was adsorbed by non-shared electrons, and then ROH was removed to complete hydrolysis [32]. The reaction process was shown in Fig. 10.

It can be found from the above hydrolysis process that the effective rate of TEOS acid-catalyzed hydrolysis process depends on the concentration of acid. The higher the concentration, the faster the hydrolysis rate. When TEOS was added in the preparation process of the aluminum sol, because the aluminum powder was not completely dissolved, the acid in the solution was in an excessive state, and the concentration of H_3O^+ was high. Therefore, the hydrolysis rate of TEOS was very fast, and silica sol can be formed in a short time. The formed silica sol does not react

with the aluminum sol to form a diphasic sol. When the prepared aluminum carboxylate sol was mixed with TEOS, the concentration of H_3O^+ in the aluminum carboxylate sol was greatly reduced, so the hydrolysis rate of TEOS was significantly reduced. At the same time, $Al(OOCH)(OOCH)(H_2O)_4^+$, $Al(OOCH)(OOC_2H_3)(H_2O)_4^+$ and other ions in the aluminum sol reacted with Si-OH, which promoted the reaction between aluminum and silicon. Therefore, aluminum and silicon were mixed at the atomic level to form a monophasic sol.

Combined with the above results and analysis, the influence mechanism of TEOS addition method on the preparation of alumina-mullite composite fibers by sol–gel method is shown in Fig. 11. The difference of precursor sol eventually leads to the difference of fibers in the sintering process. The diphasic alumina-mullite precursor sol was formed by the pre-addition of TEOS. There were no Al-O-Si linkages between Al and Si in the sol, which belonged to the physical scale mixing. Therefore, during the sintering process of the fiber, γ-Al_2O_3 was first formed, and then amorphous SiO_2 reacted with γ-Al_2O_3 to form stable orthorhombic mullite. The generated mullite inhibited the slip of grain boundaries, thereby inhibiting the growth of grains. The post-addition method of TEOS formed a monophasic aluminum-silicon sol. There were Al-O-Si linkages between aluminum and silicon in the sol, which belongs to atomic-scale mixing. During the sintering process, mullite was formed at around 800 °C dues to the presence of Al-O-Si linkages. In addition, because the mullite formation temperature was low, there was no other phase to inhibit the growth of mullite, so the grain size of the fibers sintered at high temperature was large.

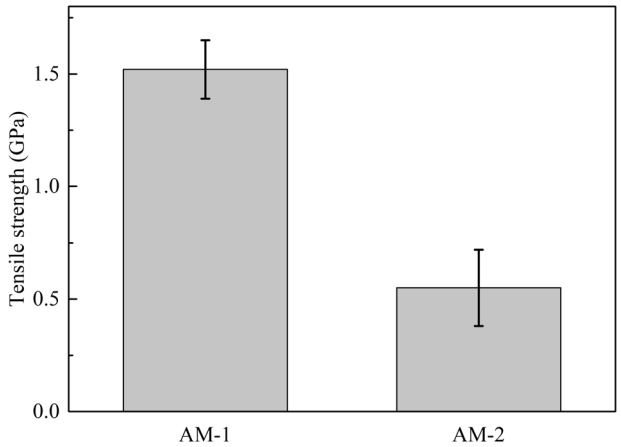

Fig. 9 Tensile strength of the alumina-mullite composite fibers sintered at 1400 °C for 5 min in air

5 Conclusion

Different aluminum-silica sols were prepared by adjusting the mixing procedure using aluminum carboxylate sol and TEOS as the aluminum source and silicon source, respectively. The effects of Al and Si mixing procedures on the phase transition and microstructure evolution of alumina-

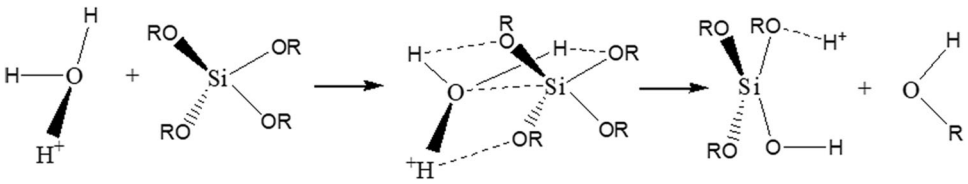

Fig. 10 Hydrolysis diagram of TEOS under acid catalysis [29]

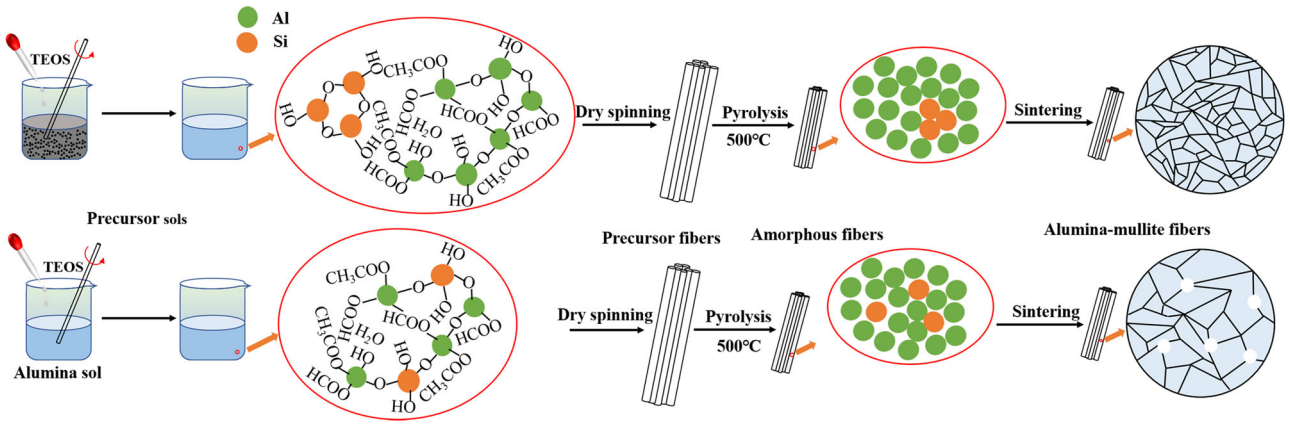

Fig. 11 The mechanism diagram of the effect of Al-Si mixing methods on the preparation of alumina-mullite composite fibers by sol–gel method

mullite composite fibers were investigated. The different mixing procedures of aluminum and silicon affect the phase transition of alumina-mullite composite fibers. The phase transition path of the fiber obtained by adding TEOS during the preparation of alumina sol was: Amorphous alumina → γ-Al_2O_3 → γ-Al_2O_3 + orthorhombic mullite → θ-Al_2O_3 + α-Al_2O_3 + orthorhombic mullite → α-Al_2O_3 + orthorhombic mullite. The phase transition path of AM-2 fibers obtained by mixing the aluminum carboxylate sol and TEOS was: Amorphous → tetragonal mullite → θ-Al_2O_3, α-Al_2O_3, tetragonal + mullite → α-Al_2O_3 + orthorhombic mullite. The different mixing procedures of aluminum and silicon also affect the morphology of alumina-mullite composite fibers. The fibers obtained by adding TEOS during the preparation of aluminum carboxylate sol showed a dense structure with fine grains after sintering at 1300 °C for 1 h, and the grains size was about 500 nm after sintering at 1400 °C for 1 h. However, after sintering at 1300 °C for 1 h, the grain size of fibers obtained by mixing aluminum carboxylate sol and TEOS was larger than 1 μm. The difference in phase transition and microstructure evolution between the two fibers obtained by different aluminum-silicon mixing procedures was that the precursor sol obtained by adding TEOS during the preparation of aluminum sol is a diphasic sol, and the precursor sol obtained by adding TEOS in the prepared aluminum carboxylate sol was a monophasic sol.

Acknowledgements The authors gratefully acknowledge the financial support from the National Nature Science Foundation of China (Project No. U20A20240).

Compliance with ethical standards

Conflict of interest The authors declare that they have no known competing financial interests or personal relationships that could have appeared to influence the work reported in this paper.

References

1. Wang W, Zhang L, Dong X, Wu J, Zhou Q, Li S, Shen C, Liu W, Wang G, He R (2022) Additive manufacturing of fiber reinforced ceramic matrix composites: advances, challenges, and prospects. Ceram Int 48(14):19542–19556
2. Belmonte M (2006) Advanced ceramic materials for high temperature applications. Adv Eng Mater 8(8):693–703
3. Schawaller D, Clauß B, Buchmeiser MR (2012) Ceramic filament fibers - a review. Macromol Mater Eng 297(6):502–522
4. Li L, Chen M, Dong Y, Dong X, Cerneaux S, Hampshire S, Cao J, Zhu L, Zhu Z, Liu J (2016) A low-cost alumina-mullite composite hollow fiber ceramic membrane fabricated via phase-inversion and sintering method. J Eur Ceram Soc 36(8):2057–2066
5. Wilson DM, Visser LR (2001) High performance oxide fibers for metal and ceramic composites. Compos Part A 32(8):0–1153
6. Li J, Wu W, Yang H, Wang X, Wang X, Sun C, Hu Z (2019) Rigid silica xerogel/alumina fiber composites and their thermal insulation properties. J Porous Mater 26(4):1177–1184
7. Krenkel W (2008) Ceramic matrix composites: fiber reinforced ceramics and their applications. John Wiley & Sons, pp. 165–186
8. Li X, Su X, Xiao H, Chen L, Li S, Tang M (2020) Continuous α-Al_2O_3 fibers grown by seeding with in-situ suspension. Ceram Int 46(10, Part A):15638–15645
9. Zamani SMM, Behdinan K (2018) Multiscale modeling of the mechanical properties of Nextel 720 composite fibers. Compo Struct 204:578–586
10. Song X, Ma Y, Wang J, Liu B, Yao S, Cai Q, Liu W (2018) Homogeneous and flexible mullite nanofibers fabricated by electrospinning through diphasic mullite sol-gel route. J Mater Sci 53(20):14871–14883
11. Li X, Xu H, Wang Q, Li S, Xiao H, Zhang L, Tang M, Chen L (2019) Control of continuous α-Al_2O_3 fibers by self-seeding and SiO_2-Sol doping. Ceram Int 45(9):12053–12059
12. Taktak Ş, Artır R, Yılmaz S, Bindal C (2004) Fracture toughness of alumina-mullite composites produced by infiltration process. Key Eng Mater 264:981–984
13. Taktak S, Baspinar M (2005) Wear and friction behaviour of alumina/mullite composite by sol-gel infiltration technique. Mater Des 26(5):459–464
14. Scholz H, Vetter J, Herborn R, Ruedinger A (2020) Oxide ceramic fibers via dry spinning process—from lab to fab. Int J Appl Ceram Technol 17(4):1636–1645
15. Yin L, Zhang Z-F, Halloran J, Laine RM (1998) Yttrium aluminum garnet fibers from metalloorganic precursors. J Am Ceram Soc 81(3):629–645
16. Schneider H, Okada K, Pask JA (1994) Mullite and Mullite Ceramic. Wiley, New York, pp. 213–240
17. Mendonca A, Ferreira J, Salvado IM (1998) Mullite-alumina composites prepared by sol-gel. J Sol Gel Sci Technol 13:201–205
18. Chakraborty AK (2005) Aluminosilicate formation in various mixtures of tetra ethyl orthosilicate (TEOS) and aluminum nitrate (ANN). Thermochim Acta 427(1):109–116
19. Sedaghat A, Taheri-Nassaj E, Soraru G, Ebadzadeh T (2011) A comparative study of microstructural development in the sol-gel derived alumina-mullite nanocomposites using colloidal silica and tetraethyl orthosilicate. J Sol Gel Sci Technol 58:689–697
20. Dong X, Liu J, Li X, Zhang X, Xue Y, Liu J, Guo A (2017) Electrospun mullite nanofibers derived from diphasic mullite sol. J Am Ceram Soc 100(8):3425–3433
21. Wu J, Lin H, Li JB, Zhan XB, Li JF (2009) Fabrication and characterization of electrospun mullite nanofibers. Mater Lett 63(27):2309–2312
22. Jiang W, Lin H, Li J, Zhan X, Li J (2010) Synthesis and characterization of electrospun mullite nanofibers. Adv Eng Mater 12(1-2):71–74
23. Nýblová D, Senna M, Düvel A, Heitjans P, Billik P, Filo J, Šepelák V (2019) NMR study on reaction processes from aluminum chloride hydroxides to alpha alumina powders. J Am Ceram Soc 102(5):2871–2881
24. Jaymes I, Douy A (1996) New aqueous mullite precursor synthesis. Structural study by ^{27}Al and ^{29}Si NMR spectroscopy. J Eur Ceram Soc 16(2):155–160
25. Liu Q, Wu C, Zhan L, Liu W, Yao S, Wang J, Ma Y (2023) Effect of residual carbon on the phase transformation and microstructure evolution of alumina-mullite fibers prepared by sol-gel method. J Eur Ceram Soc 43(3):1039–1050
26. Cividanes LS, Campos T, Rodrigues LA, Brunelli DD, Thim GP (2010) Review of mullite synthesis routes by sol-gel method. J Sol Gel Sci Technol 55(1):111–125

27. Wei WC, Halloran JW (1988) Transformation kinetics of diphasic aluminosilicate gels. J Am Ceram Soc 71(7):581–587
28. Li C, Liu W, Luo T, Cheng M, Liu Q, Wang J, Yao S, Ma Y (2021) Effect of formic-acid-to-acetic-acid ratio on the structure and spinnability of aqueous aluminium sol of alumina fibre. Ceram Int 47(18):26034–26041
29. Brinker CJ, Scherer GW (2013) Sol-gel science: the physics and chemistry of sol-gel processing. Academic press, pp. 45–69
30. Chen X, Gu L (2009) Sol-gel dry spinning of mullite fibers from AN/TEOS/AIP system. Mater Res Bull 44(4):865–873
31. Harris MT, Brunson RR, Byers CH (1990) The base-catalyzed hydrolysis and condensation reactions of dilute and concentrated TEOS solutions. J Non Cryst Solids 121(1-3):397–403
32. Rubio F, Rubio J, Oteo J (1998) A FT-IR study of the hydrolysis of tetraethylorthosilicate (TEOS). Spectrosc Lett 31(1):199–219